Electronic Supplementary Material (ESI) for Journal of Materials Chemistry A.

Supporting Information

Low-cost *p*-Benzoquinone-formaldehyde Polymer/Reduced Graphene Oxide Composite Film for Cathode Material of Rechargeable Lithium-ion Battery

Zhouqishuo Cai, Jinmeng Zhang, Zewen Lin, Yanan Zhao, Qianqian Yang, Xiaowen Qiu, Shumin Lin, Donghua Liu, Xiaolan Hu, Hua Bai*

College of Materials, Xiamen University, Xiamen 361005, P R China

E-mail addresses: baihua@xmu.edu.cn

Table of Contents

Page No.

Experimental section

S1. Materials

All chemical reagents were perchased from commercial sources without further purification. Al foil (Jinghong New Energy, Battery), Celgard 2500 (Jinghong New Energy, Battery), Graphite powder (Shanghai Acmec Biochemical, 45 μm, 99.95%), Hydroquinone (Shanghai Acmec Biochemical, 99%), Li (Jinghong new energy, Battery), Lithium iron(II) phosphate (Macklin, 98%), Potassium bromide (Huiyao Xingye Science and Technology, SP), Potassium permanganate (Xilong Chemical, AR), PVDF (Aladdin, Battery), s - Trioxane (Adamas-beta, 99%+):, Super-P (Jinghong New Energy, Battery), Ammonia solution (Sinopharm Chemical, AR), Dimethyl Sulfoxide-D6 (Adamas-beta, 99.9%), Electrolyte (Duoduo Chemical, 1.0 M $LiPF_6$ in EC:DMC (1:1 by volume), 1.0 M $LiPF_6$ in EC:DEC (1:1 by weight) with 1.0% VC, 1.0 M LiTFSI in DOL:DME (1:1 by volume)), H_2O (home-made), Hydrochloric acid (Xilong Chemical, AR), Hydrazine hydrate (Xilong Chemical, CP), Hydrogen peroxide (Xilong Chemical, AR), 1-Methyl-2-pyrrolidinone (Aladdin, GC), Sulfuric acid (Xilong Chemical, AR), Ar (Xinhang Industrial, 99.999%).

S2. Synthesis of *p*-benzoquinone-formaldehyde copolymer (FQ)

10 mL of deionized water, 5 mL of concentrated hydrochloric acid (37%), and 0.6 g of paraformaldehyde were added sequentially into a three-necked flask and reacted in a water bath at 50 ℃ for 1.5 h. Under the protection of argon, 10 mL of deionized water, 2.2 g of hydroquinone were added into the flask, and the mixture was heated at 60 ℃ for 24 h. After filtration and washing with pure water, 2.25 g of brown powder was obtained, with a yield of 92.2%.

S3. Synthesis of FQ/rGO composite films

GO and rGO hydrogel were prepared following the procedure in previous reference.[1] To prepare FQ/rGO composite films, 5 mL of deionized water, 2 mL of concentrated

hydrochloric acid (37%), and 30 mg of polyformaldehyde were sequentially added to a three-necked flask and reacted in a water bath at 50 ℃ for 1.5 h. Under argon protection, 20 g GO aqueous solution (3.3 mg g^{-1}) and 110 mg of hydroquinone were added, and the reaction was carried out at 60 ℃ for 24 h. 5 mL of ammonia, 100 μL of hydrazine hydrate (80 wt%) were then added, and the reaction was carried out at 90 ℃ in an oil bath for 1.5 h. After cooling down to room temperature, the obtained black flocculent was diluted by 800 mL of deionized water and filtered through a PVDF film (220 nm), yielding the FQ/rGO composite films.

S4. Assembly of coin cells

FQ or LFP, Super P, and PVDF (mass ratio: 2.5:6.5:1 for FQ, 8:1:1 for LFP) were placed in an onyx mortar and ground for 10 min to obtain a homogeneous mixture. The mixed powder was transferred to a small glass vial, and an appropriate amount of NMP was added as a solvent and magnetically stirred for 24 h to obtain a homogeneous slurry. The slurry was uniformly coated on a clean aluminum foil using a spatula and vacuum dried at 75 ℃ for 12 h. The cathode sheets were obtained.

The coin cell LIR 2032 type used in this experiment was assembled in a glove box filled with dry argon gas, the water-oxygen values inside the glove box were all less than 0.01 ppm during the assembly process. FQ electrode sheets, FQ/rGO composite films, or LFP electrode sheets were cut into electrode sheets with a diameter of 12 mm. The lithium tablets were used as the anodes, 1.0 M $LiPF_6$ in EC/DEC (1:1 vol%, EC: ethylene carbonate, DEC: diethyl carbonate) was used as the electrolyte, and Celgard 2500 was used as the separator. The batteries were allowed to stand for 5 hours and then subjected to a series of electrochemical performance tests. All electrochemical performance tests except low-temperature tests were conducted at 26 ℃.

S5. Electrode immersion

FQ electrode sheets and FQ/rGO composite films were cut into electrode sheets with a

diameter of 12 mm. Then, FQ electrode sheets and FQ/rGO composite films were immersed into the electrolytes (1.0 M $LiPF_6$ in 1:1 (in volume) EC/DEC and 1.0 M LiTFSI in 1:1 (in volume) DOL/DME, EC: ethylene carbonate, DEC: diethyl carbonate), DOL: dioxolane, DME: ethylene glycol dimethyl ether) for 30 days. Besides, the FQ/rGO coin cells were discharged to 1.5 V after 5 cycles of charge/discharge at the current density of 100 mA g^{-1}, disassembled, and FQ/rGO films in the discharged state were achieved. Then the FQ/rGO films in the discharged state were immersed in 1.0 M LiPF6 in EC/DEC for 30 days.

S6. Electrochemical characterization

FQ/rGO composite films, LFP, and FQ sheets as cathode material were directly assembled into cells, and the two-electrode cyclic voltammetry test was performed on CHI 760E electrochemical workstation with a scan rate of 5 mV s^{-1}. The cells were subjected to constant current charge/discharge tests on Wuhan Lanhe CT2001A battery test system. FQ/rGO-b, FQ/rGO-c, and FQ/rGO-d were tested at a voltage range of 1.5 ~ 4.0 V with a current of 40 μA. The current densities of cyclic stability tests were 170 mA g^{-1}, 500 mA g^{-1}, 1000 mA g^{-1} and 2500 mA g^{-1}, and that of rate tests were 500 mA g^{-1}, 1000 mA g^{-1}, 2000 mA g^{-1}, 5000 mA g^{-1} and 10000 mA g^{-1}, current densities for electrolyte test, and low-temperature test were 2500 mA g^{-1}.

S7. Material characterization

NMR ^1H spectra was collected on Avance II 400M spectrometer (Bruker, Germany). IR spectrum were measured on Nicolet IS 10 infrared spectrometer (ThermoFisher, USA) with athe ATR mode (Ge crystal). The morphology of samples were observed using a scanning electron microscope SU-70 (Hitachi, Japan). and a TALOS F200 tranmission electron microscope (FEI, USA). Thermogravimetic curves were measured on a Ultra-high temperature simultaneous thermal analyzer Setsys Evolution18 (Sertaram Instruments, France). Fully automated specific surface and microporous analyzer 3H-2000PM2 (Best Instrument Technology, China) was used to analyze the

specific surface area and pore size distribution of the composite films. XRD patterns were obtained on an X-ray diffractometer D8-A25 (Bruker, USA). X-ray photoelectron spectroscopy (XPS) spectra were recorded using a Quantum 2000 XPS system (Physical Electronics, USA).

S8. Calculation of theoretical specific capacity of polymer FQ

The maximum theoretical specific capacity of polymer FQ (C, 446 mAh g^{-1}) can be calculated according to the following formula.

$$C = \frac{nN_Ae}{3600 \times \frac{M_R}{1000}}$$

Here, n is the amount of lithium ions (2 mol) that can be inserted in 1 mol of active material, N_Ae is Faraday's constant (96485 C mol^{-1}), M_R is the relative molecular mass of a structural unit, which ranges between 120 ~ 132 g mol^{-1}, taking into account that the benzene ring may be connected with one or two methylene groups.

S9. Calculation of the content of FQ in FQ/rGO.

The content of FQ (x) in the composite film can be calculated according to the following formula.

$$x = \frac{FQ/rGO - rGO}{FQ - rGO} \times 100\%$$

Here, *FQ/rGO* is the percentage of mass loss of the composite films at 400-700 °C, rGO is the percentage of mass loss of *rGO* at 400-700 °C, *FQ* is the percentage of mass loss of the polymer at 400-700 °C.

S10. The cost of FQ/rGO composite films and LFP electrode in laboratory.

All reagent prices come from the website (aladdin-e.com). The cost of solvents is not calculated for ease of comparison with other works.

LFP:

Super-P: $ 370/kg, PVDF: $ 237.8/kg, LFP: $ 143.7/kg.

The cost of preparing 1 kg of LFP electrode material blend (LFP/carbon black/binder = 8:1:1) is:

$$143.7 \times 0.8 + 237.8 \times 0.1 + 370 \times 0.1 = 175.7 \text{ \$}$$

The theoretical cost of the electrode providing 1 Ah is;

$$\frac{175.7}{170 \times 0.8} = 1.03 \text{ \$}$$

At a current density of 500 mA g^{-1}, the cost of the electrode providing 1 Ah is (Fig. S16):

$$\frac{175.7}{69.3 \times 0.8} = 3.17 \text{ \$}$$

At a current density of 1000 mA g^{-1}, the cost of the electrode providing 1 Ah is (Fig. S16):

$$\frac{175.7}{53.7 \times 0.8} = 4.09 \text{ \$}$$

FQ/rGO composite films:

$N_2H_4 \cdot H_2O$ (80 wt%): $ 88.7/L, $KMnO_4$: $ 16.2/kg, H_2SO_4 (98%): $ 4/L, H_2O_2 (30%): $ 4.6/L, HCl (37%): $ 3.2/L, graphite powder (45 μm): $ 26.52/kg, trimeric formaldehyde: $ 11.67/kg, hydroquinone: $ 34.0/kg.

If 1 kg of graphite powder is used, 1.5 kg of GO are produced. The cost of preparing 1 kg of GO is:

$$\frac{2}{3} \times (1 \times 26.52 + \frac{9}{3} \times 16.2 + \frac{70}{3} \times 4 + \frac{15}{3} \times 4.6 + \frac{25}{3} \times 3.2) = 144 \text{ \$}$$

In FQ/rGO composite films, the content of rGO is 71.3%. After GO is restored, the resulting rGO is 66% of its original quality. According to the feeding ratio of preparing FQ/rGO composite films, the cost of preparing 1 kg of FQ/rGO is:

$$\frac{0.713}{0.66}\times(1\times144+\frac{30}{66}\times11.67+\frac{110}{66}\times34.0+\frac{100}{66}\times88.7)=368\ \$$$

The theoretical cost of the electrode providing 1 Ah is；

$$\frac{368}{446\times0.287}=2.87\ \$$$

At a current density of 500 mA g^{-1}, the cost of the electrode providing 1 Ah is (Fig. 4b):

$$\frac{368}{464.7\times0.287}=2.76\ \$$$

At a current density of 1000 mA g^{-1}, the cost of the electrode providing 1 Ah is (Fig. 4b):

$$\frac{368}{437.7\times0.287}=2.93\ \$$$

S11. The cost of commercialized FQ/rGO composite films and LFP electrode.

The costs of FQ/rGO films and LFP were recalculated, and all reagent prices come from Changjiang Securities.

LFP electrode:

Super-P: \$ 3893/t, PVDF: \$ 8204/t, LFP: \$ 5770/t, NMP: \$ 1641/t (1.03×10^3 kg m^{-3}), Al foil: \$ 4714/t (2.7×10^3 kg m^{-3}, 20 μm).

The cost of preparing 1 kg of LFP electrode material blend (LFP/carbon black/binder = 8:1:1) is:

$$5.77\times0.8+3.893\times0.1+8.204\times0.1=5.826\ \$$$

If the cost of Al foil and NMP is taken into consideration the ratio of PVDF to NMP is 60 mg:1 mL, the energy density is 1 mAh cm^{-2}, the total cost is:

$$5.826+\frac{100}{60}\times1.641\times1.03+4.714\times2.7\times20\times10^{-9}\times\frac{170\times0.8\times1000}{10000}=8.64\ \$$$

At a current density of 500 mA g^{-1}, the cost of providing 1 Ah is (Fig. S16):

$$\frac{8.64}{69.3\times0.8}=0.156\ \$$$

At a current density of 1000 mA g^{-1}, the cost of providing 1 Ah is (Fig. S16):

$$\frac{8.64}{53.7\times0.8}=0.201\ \$$$

FQ/rGO composite films:

$NH_3{\cdot}H_2O$: \$ 431/t (0.91×10^3 kg m^{-3}), $N_2H_4{\cdot}H_2O$ (80 wt%): \$ 2224/t (1.03×10^3 kg m^{-3}), $KMnO_4$: \$ 2155/t, H_2SO_4 (98%): \$ 73.7/t (1.84×10^3 kg m^{-3}), H_2O_2 (30%): \$ 116.9/t (1.11×10^3 kg m^{-3}), HCl (37%): \$ 21.3/t (1.19×10^3 kg m^{-3}), graphite powder (45 μm): \$ 553/t, trimeric formaldehyde: \$ 2781/t, hydroquinone: \$ 5006/t.

If 1 kg of graphite powder is used, 1.5 kg of GO are produced. The cost of preparing 1 kg of GO is:

$$\frac{2}{3}\times(1\times0.553+\frac{9}{3}\times2.155+\frac{70}{3}\times0.0737\times1.84+\frac{15}{3}\times0.1169\times1.11+\frac{25}{3}\times0.0213\times1.19)=7.36\ \$$$

In FQ/rGO composite films, the content of rGO is 71.3%. After GO is reduced, the produced rGO is 66% of the original mass of GO. According to the feeding ratio of preparing FQ/rGO composite films, the cost of preparing 1 kg of FQ/rGO is:

$$\frac{0.713}{0.66}\times(1\times7.36+\frac{30}{66}\times2.718+\frac{110}{66}\times5.006+\frac{100}{66}\times2.224\times1.03+\frac{2000}{66}\times0.0213\times1.19+\frac{5000}{66}\times0.431\times0.91)=55.0\ \$$$

At a current density of 500 mA g^{-1}, the cost of providing 1 Ah is (Fig. 4b):

$$\frac{55.0}{464.7\times0.287}=0.412\ \$$$

At a current density of 1000 mA g^{-1}, the cost of providing 1 Ah is (Fig. 4b):

$$\frac{55.0}{437.7\times0.287}=0.438\ \$$$

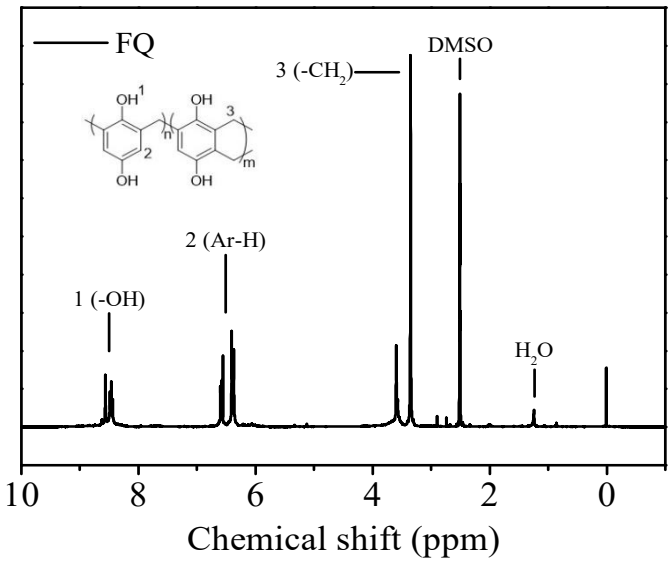

Fig. S1. ^{1}H NMR spectra of FQ (polymer), ^{1}H NMR (400 MHz，DMSO – D6), 8.50 (m, 2H), 6.48 (m, 2H), 3.49 (m, 2H).

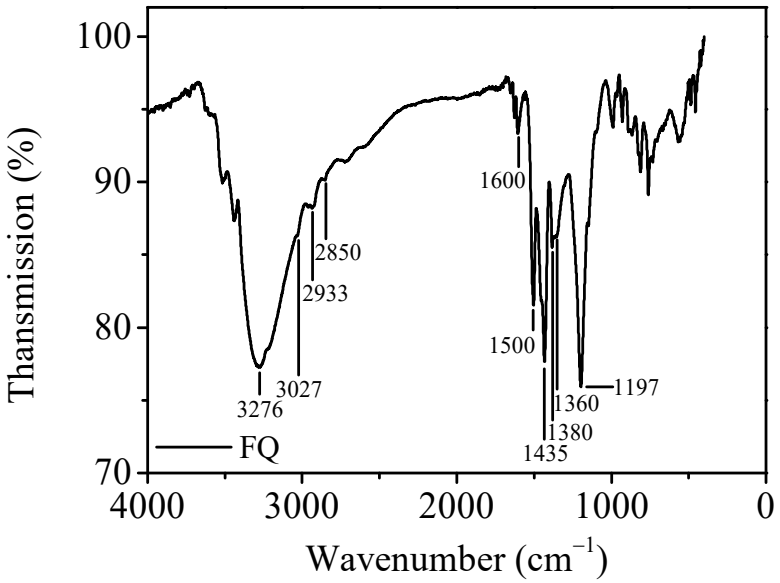

Fig. S2. IR spectra of FQ.

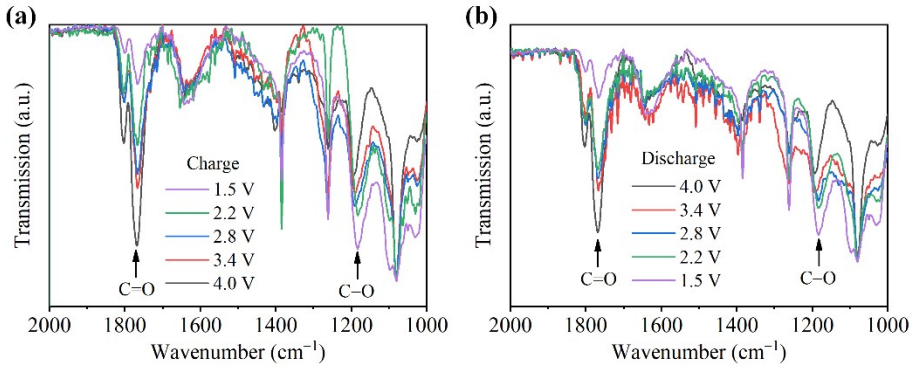

Fig. S3. IR spectra of FQ at different (a) charge, (b) discharge voltages

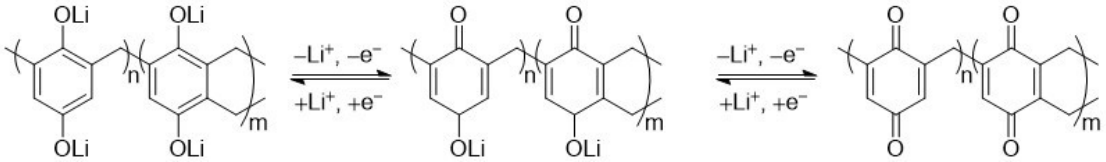

Scheme S1. Principle of charge and discharge reactions

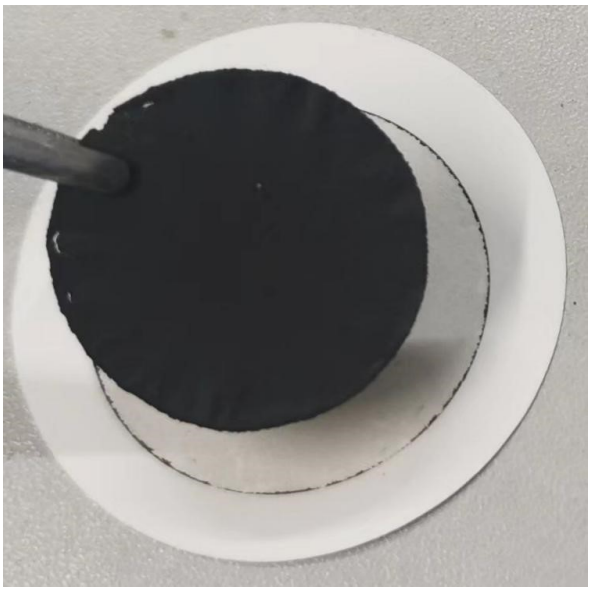

Fig. S4. The picture of FQ/rGO composite films

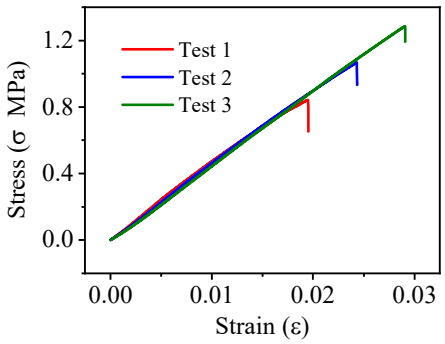

Fig. S5. Typical stress-strain curve of FQ/rGO composite films

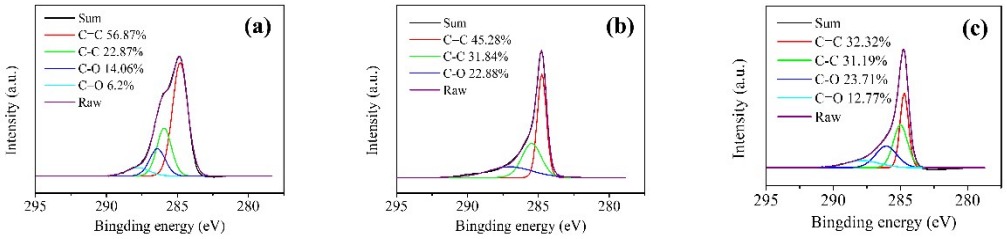

Fig. S6. XPS patterns of (a) FQ, (b) rGO, and (c)FQ/rGO

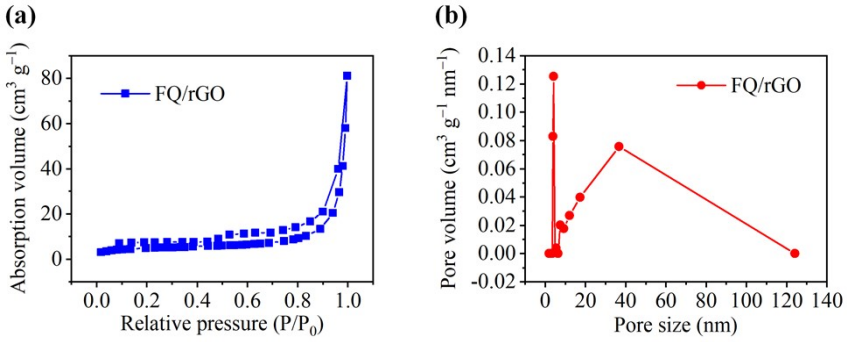

Fig. S7. BET test of FQ/rGO (a) N_2 adsorption/desorption curve, (b) pore size profile

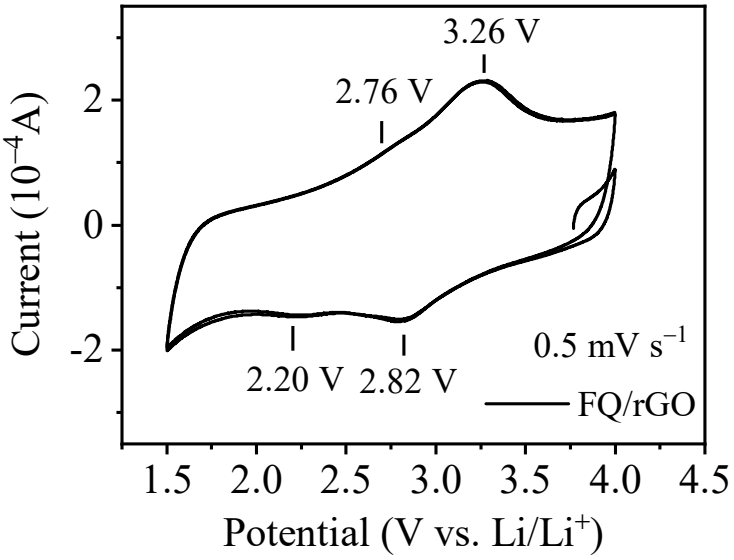

Fig. S8. CV curve of FQ/rGO (V. vs Li^+/Li)

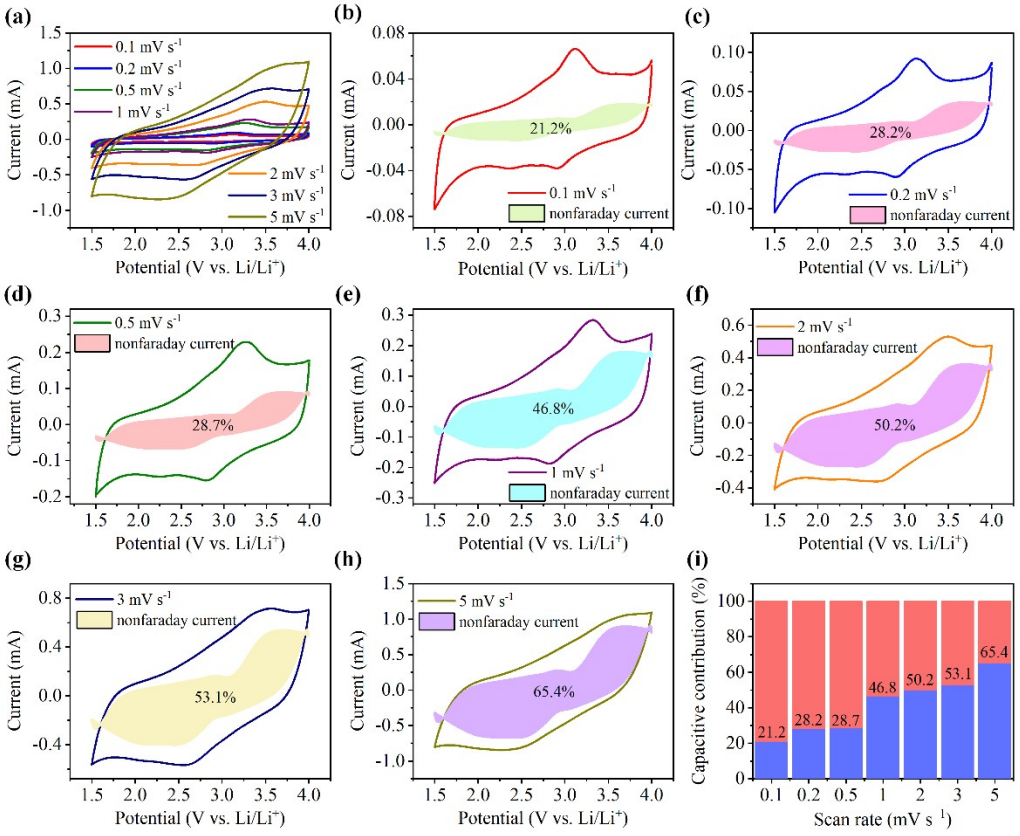

Fig. S9. (a) CV curve of FQ/rGO (V. vs Li^+/Li) at different scan rates (0.1, 0.2, 0.5, 1, 2, 3, 5 mV s^{-1}). (b ~ h) CV curves of contribution ratio of capacitive energy storage at

scan rates of 0.1 mV s^{-1} (b), 0.2 mV s^{-1} (c), 0.5 mV s^{-1} (d), 1 mV s^{-1} (e), 2 mV s^{-1} (f), 3 mV s^{-1} (g), 5 mV s^{-1} (h). (i) A histogram of contribution ratio of capacitive energy storage at different scan rates.

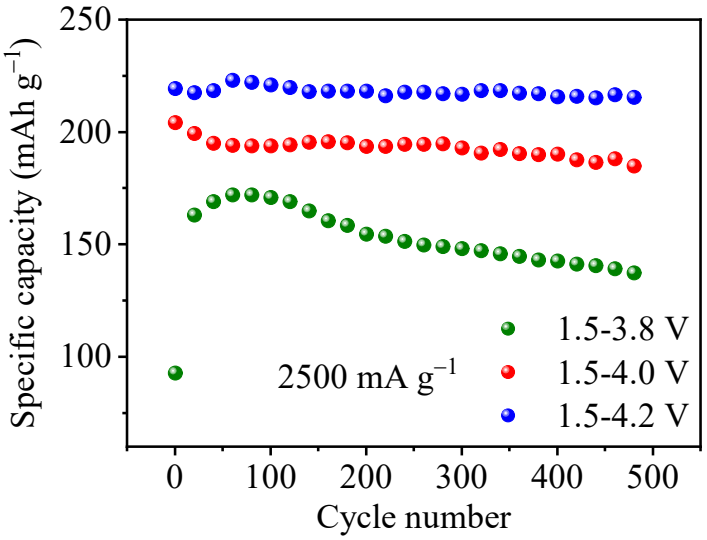

Fig. S10. Specific capacity of FQ/rGO at different potential ranges

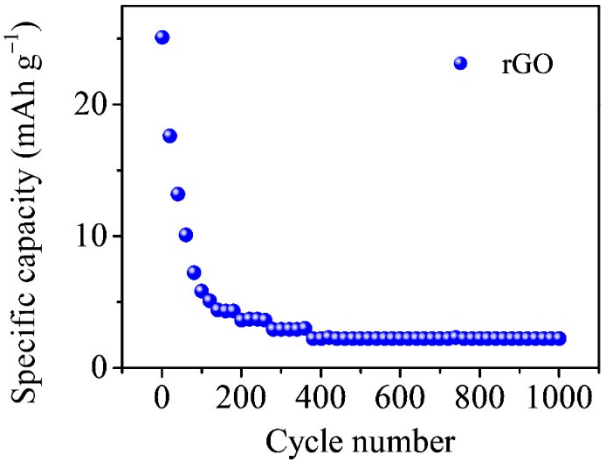

Fig. S11. Cycle test of pure rGO

Fig. S12. The pictures of randomly selected and disassembled cells after long cycle tests

Fig. S13. Image of discharged FQ/rGO films immersed in DMC for 30 days

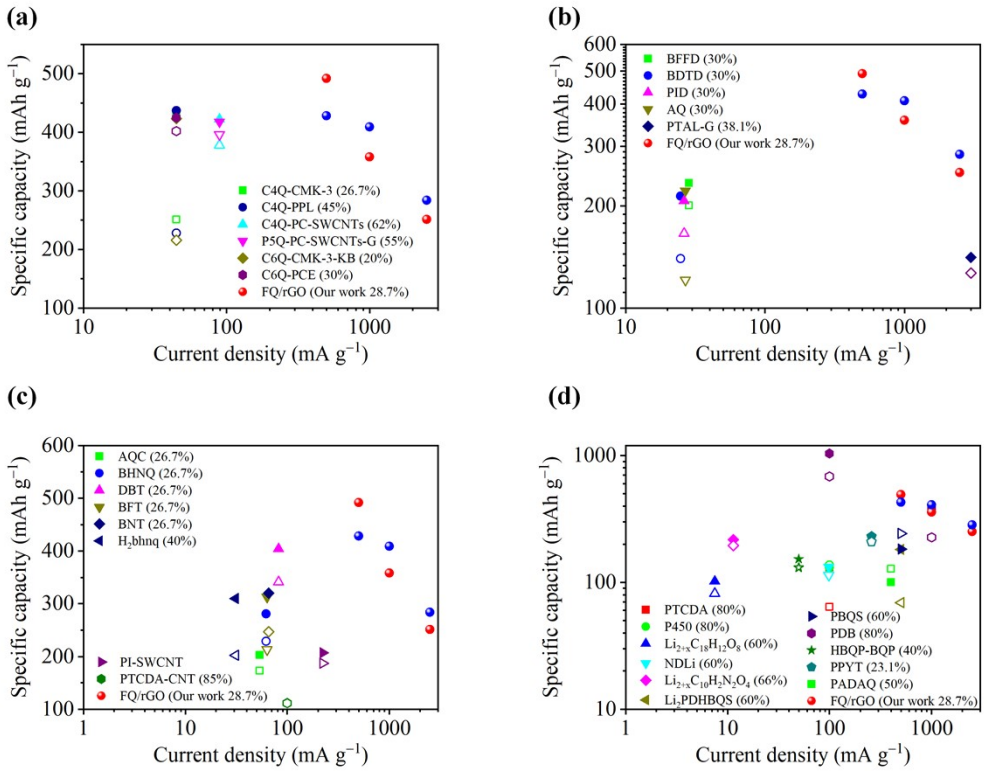

Fig. S14. In terms of cyclic stability, our work is compared with a) other electrode materials with the same electroactive unit (all with theoretical specific capacities of

446 mAh g^{-1}), b) carbonyl material/rGO composites, c) carbonyl material/carbon material composites, and d) other carbonyl materials. [2-7] [8-17] [18-21] [22-25]

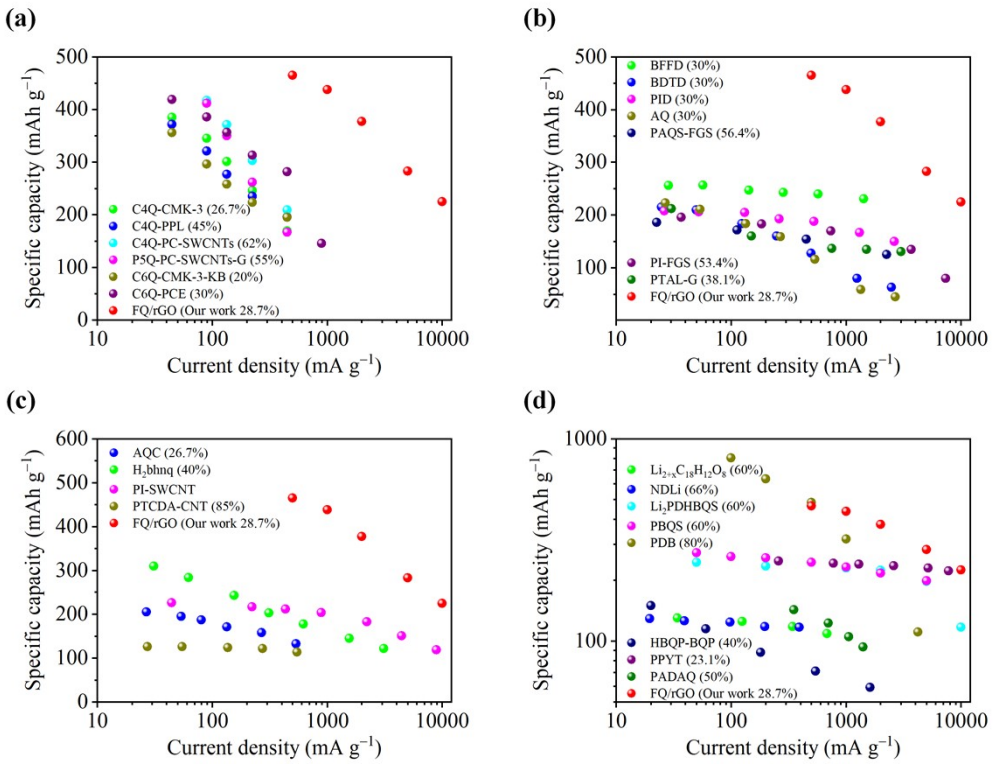

Fig. S15. In terms of rate performance, our work is compared with a) other electrode materials with the same electroactive unit (all with theoretical specific capacities of 446 mAh g^{-1}), b) carbonyl material/rGO composites, c) carbonyl material/carbon material composites, and d) other carbonyl materials.

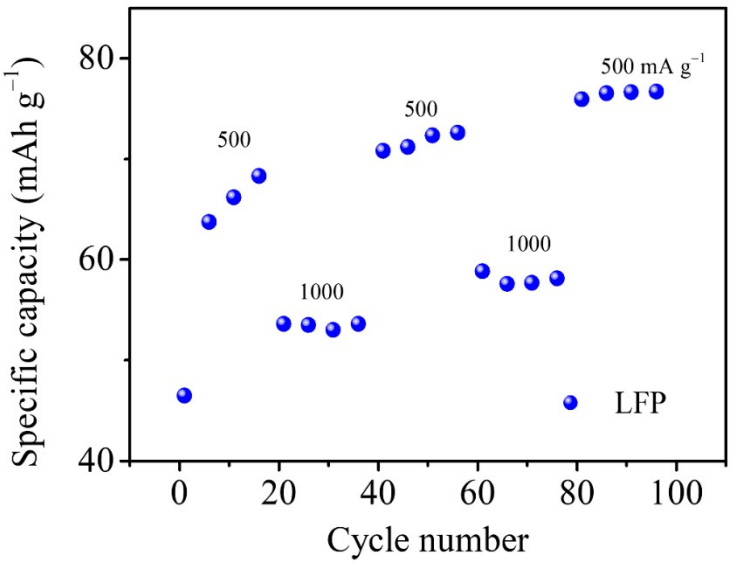

Fig. S16. Rate performance of LFP

Table S1. Ratio of the hydroquinone, polyformaldehyde and GO

	Hydroquinone [mg]	Polyformaldehyde [mg]	GO [mg]
FQ/rGO-a	55	15	66
FQ/rGO-b	110	30	66
FQ/rGO-c	220	60	66
FQ/rGO-d	330	90	66

Table S2. Summary for the costs of carbonyl compounds in laboratory

	Production cost [$/kg]	Content of active material [%]	Production cost (related to the total mass of electrode) [$/A h]	Ref.
FQ/rGO	368	28.7	2.76	Our work
NP2	480	30	6.33	[26]

PDBS	1505	60	71.67	[27]
PAQS	636	40	80.25	[28]
P15AQ	6017	60	477.5	[29]
P14AQ	55800	60	3536.2	[29]
PADAQ	110	50	21.8	[9]
PDHBQS	2457	70	195	[30]
Polyimide	205	5	432	[31]
DHAP	129	30	130.3	[32]
PI-3	1303	60	133.2	[33]
NT	1195	60	113.8	[34]
UP	199	60	41.5	[35]
BBQ	3197	60	181.8	[36]
BBQB	1648	60	74.8	[36]

Reference

1. J. Chen, B. W. Yao, C. Li and G. Q. Shi, *Carbon*, 2013, **64**, 225-229.
2. S. Zheng, H. Sun, B. Yan, J. Hu and W. Huang, *Sci. China Mater.*, 2018, **61**, 1285-1290.
3. W. Huang, Z. Zhu, L. Wang, S. Wang, H. Li, Z. Tao, J. Shi, L. Guan and J. Chen, *Angew. Chem. Int. Ed.*, 2013, **52**, 9162-9166.
4. W. Huang, M. Zhang, H. Cui, B. Yan, Y. Liu and Q. Zhang, *Chem-asian. J.*, 2019, **14**, 4164-4168.
5. W. Huang, X. Zhang, S. Zheng, W. Zhou, J. Xie, Z. Yang and Q. Zhang, *Sci. China Mater.*, 2020, **63**, 339-346.
6. W. Huang, S. Zheng, X. Zhang, W. Zhou, W. Xiong and J. Chen, *Energy Storage Mater.*, 2020, **26**, 465-471.
7. Z. Zhu, M. Hong, D. Guo, J. Shi, Z. Tao and J. Chen, *J. Am. Chem. Soc.*, 2014, **136**, 16461-16464.
8. K. Pirnat, G. Mali, M. Gaberscek and R. Dominko, *J. Power Sources*, 2016, **315**, 169-178.
9. L. Zhao, W. Wang, A. Wang, K. Yuan, S. Chen and Y. Yang, *J. Power Sources*, 2013, **233**, 23-27.
10. Z. Song, Y. Qian, T. Zhang, M. Otani and H. Zhou, *Adv. Sci.*, 2015, **2**, 1500124.
11. J. Xie, Z. Wang, P. Gu, Y. Zhao, Z. J. Xu and Q. Zhang, *Sci. China Mater.*, 2016, **59**, 6-11.
12. T. Nokami, T. Matsuo, Y. Inatomi, N. Hojo, T. Tsukagoshi, H. Yoshizawa, A. Shimizu, H. Kuramoto, K. Komae, H. Tsuyama and J.-i. Yoshida, *J. Am. Chem. Soc.*, 2012, **134**, 19694.
13. X. Han, C. Chang, L. Yuan, T. Sun and J. Sun, *Adv. Mater.*, 2007, **19**, 1616-+.

14. S. Renault, J. Geng, F. Dolhem and P. Poizot, *Chem. Commun.*, 2011, **47**, 2414-2416.
15. W. Walker, S. Grugeon, O. Mentre, S. Laruelle, J.-M. Tarascon and F. Wudl, *J. Am. Chem. Soc.*, 2010, **132**, 6517-6523.
16. Z. Song, Y. Qian, X. Liu, T. Zhang, Y. Zhu, H. Yu, M. Otani and H. Zhou, *Energy Environ. Sci.*, 2014, **7**, 4077-4086.
17. D. J. Kim, S. H. Je, S. Sampath, J. W. Choi and A. Coskun, *RSC Adv.*, 2012, **2**, 7968-7970.
18. Y. Liang, P. Zhang, S. Yang, Z. Tao and J. Chen, *Adv. Energy Mater.*, 2013, **3**, 600.
19. K. Pirnat, J. Bitenc, I. Jerman, R. Dominko and B. Genorio, *Chemelectronchem*, 2014, **1**, 2131-2137.
20. Z. Song, T. Xu, M. L. Gordin, Y.-B. Jiang, I.-T. Bae, Q. Xiao, H. Zhan, J. Liu and D. Wang, *Nano Lett.*, 2012, **12**, 2205-2211.
21. Q. Yu, D. Chen, J. Liang, Y. Chu, Y. Wu, W. Zhang, Y. Li and R. Zeng, *RSC Adv.*, 2014, **4**, 59498-59502.
22. K. Zhang, C. Guo, Q. Zhao, Z. Niu and J. Chen, *Adv. Sci.*, 2015, **2**, 1500018.
23. H. Li, W. Duan, Q. Zhao, F. Cheng, J. Liang and J. Chen, *Inorg. Chem. Front.*, 2014, **1**, 193-199.
24. H. Wu, S. A. Shevlin, Q. Meng, W. Guo, Y. Meng, K. Lu, Z. Wei and Z. Guo, *Adv. Mater.*, 2014, **26**, 3338-+.
25. H. Wu, K. Wang, Y. Meng, K. Lu and Z. Wei, *J. Mater. Chem. A*, 2013, **1**, 6366-6372.
26. C. Li, X. Liu, Z. He, W. Tao, Y. Zhang, Y. Zhang, Y. Jia, H. Yu, Q. Zeng, D. Wang, J. H. Xin, C. Duan and F. Huang, *J. Power Sources*, 2021, **511**, 230464.
27. K. Liu, J. Zheng, G. Zhong and Y. Yang, *J. Mater. Chem. A*, 2011, **21**, 4125-4131.
28. Z. Song, H. Zhan and Y. Zhou, *Chem. Commun.*, 2009, DOI: 10.1039/b814515f, 448-450.
29. Z. Song, Y. Qian, M. L. Gordin, D. Tang, T. Xu, M. Otani, H. Zhan, H. Zhou and D. Wang, *Angew. Chem. Int. Ed.*, 2015, **54**, 13947-13951.
30. K. Amin, Q. Meng, A. Ahmad, M. Cheng, M. Zhang, L. Mao, K. Lu and Z. Wei, *Adv. Mater.*, 2018, **30**, 1703868.
31. K. Oyaizu, A. Hatemata, W. Choi and H. Nishide, *J. Mater. Chem. A*, 2010, **20**, 5404-5410.
32. N. Zindy, J. T. Blaskovits, C. Beaumont, J. Michaud-Valcourt, H. Saneifar, P. A. Johnson, D. Belanger and M. Leclerc, *Chem. Mater.*, 2018, **30**, 6821-6830.
33. Z. Song, H. Zhan and Y. Zhou, *Angew. Chem. Int. Ed.*, 2010, **49**, 8444-8448.
34. C. Chen, X. Zhao, H.-B. Li, F. Gan, J. Zhang, J. Dong and Q. Zhang, *Electrochim. Acta*, 2017, **229**, 387-395.
35. P. Sharma, D. Damien, K. Nagarajan, M. M. Shaijumon and M. Hariharan, *J. Phys. Chem. Lett.*, 2013, **4**, 3192-3197.
36. J. Yang, P. Xiong, Y. Shi, P. Sun, Z. Wang, Z. Chen and Y. Xu, *Adv. Funct. Mater.*, 2020, **30**, 1909597.